were processed using "Biosuplar-2" software (version 2.2.30) on a PC computer. The experimental SPR reflectance curves of the polymer film were fitted with the full Fresnel equations in the six-phase model using the Nelder-Mead algorithm of minimization [36]. Cyclic voltammetry and constant potential electrolysis experiments were performed using an electrochemical analyzer (EG&G, VersaStat) linked to a computer (EG&G software #270/250). An open electrochemical cell (230 μL) enabled the easy and rapid removal and exchange of solution above the polymer films. Argon was passed through the funnel placed above the open cell to create an inert atmosphere. Glass supports (TF-1 glass, 20 mm × 20 mm) coated with a Cr sublayer (5 nm) and polycrystalline Au layer (50 nm) supplied by Analytical-μSystem, Germany, were used for the in-situ electrochemical/SPR measurements [37,38]. The Au-coated glass plate was used as a working electrode (1.5 cm^2 area exposed to the solution), an auxiliary Pt and a quasi-reference Ag electrode were made from wires 0.5 mm in diameter and added to the cell. The Ag-quasi-reference electrode was calibrated [39] by referencing to the potential of dimethylviologen, $E^{\circ} = -0.687$ V vs. SCE, measured by cyclic voltammetry, and the potentials are reported vs. SCE. The SPR-reflectance curves and their time-dependent changes were measured in situ upon application of an external potential to the working electrode.

A polyacrylic acid film was electrochemically produced on the Au-SPR electrode [25–27]. The electropolymerization was performed in an aqueous solution composed of acrylic acid, 2 M, bis-acrylamide, 0.04 M, and $ZnCl_2$, 0.2 M (pH 7.0 adjusted with NaOH). The electrode was preconditioned at the potential of –1.5 V for 10 s, then five potential cycles were applied between –1.5 V and 0.1 V (50 mV s^{-1}) and the cycling was finished at a potential of 0.1 V. The polyacrylic acid modified electrode was treated with HCl, 0.1 M, for 2 min to ensure complete dissolution of Zn^0 produced upon polymerization, the electrode was carefully washed with distilled water to remove excess monomer and Zn^{2+} ions, and subsequently treated with $CuSO_4$ solution, 0.2 M, for 30 min. The $CuSO_4$ solution was removed from the cell and the polymeric film, saturated with Cu^{2+} ions, was washed with water and 0.1 M tris-buffer (tris = tris(hydroxymethyl)aminomethane), pH 5.5, and was added to the cell as electrolyte solution.

The potential-controlled absorption features of the Cu^0/Cu^{2+}/PAA-modified Au electrode were measured with a Uvikon 860 (Kontron) spectrophotometer using a spectroelectrochemical cell composed of a cuvette with the modified working electrode, a Pt counter electrode, and Ag quasi-reference electrode connected to the potentiostat.

Received: May 10, 2002
Final version: August 1, 2002

[1] D. M. Burland, R. D. Miller, C. A. Walsh, *Chem. Rev.* **1994**, *94*, 31.
[2] I. M. Fouda, *J. Appl. Polym. Sci.* **2001**, *81*, 3349.
[3] S. Walheim, E. Schaffer, J. Mlynek, U. Steiner, *Science* **1999**, *282*, 520.
[4] W. Feng, T. R. Zhang, Y. Liu, L. Wei, R. Lu, T. J. Li, Y. Y. Zhao, J. N. Yao, *J. Mater. Res.* **2002**, *17*, 133.
[5] D. R. Rosseinsky, R. J. Mortimer, *Adv. Mater.* **2001**, *13*, 783.
[6] S. Arman, *J. New Mater. Electrochem. Syst.* **2001**, *4*, 173.
[7] P. M. S. Monk, R. J. Mortimer, D. R. Rosseinsky, *Electrochromism: Fundamentals and Applications*, VCH, Weinheim **1995**.
[8] J. G. Grote, J. S. Zetts, R. L. Nelson, F. K. Hopkins, L. R. Dalton, C. Zhang, W. H. Steier, *Opt. Eng.* **2001**, *40*, 2464.
[9] R. H. Friend, *Pure Appl. Chem.* **2001**, *73*, 425.
[10] W. H. Steier, A. Chen, S. S. Lee, S. Garner, H. Zhang, V. Chuyanov, L. R. Dalton, F. Wang, A. S. Ren, C. Zhang, G. Todorova, A. Harper, H. R. Fetterman, D. T. Chen, A. Udupa, D. Bhattachrya, B. Tsap, *Chem. Phys.* **1999**, *245*, 487.
[11] A. Donaldson, *J. Phys. D: Appl. Phys.* **1991**, *24*, 785.
[12] L. Lucchetti, F. Simoni, *Rivista Del Nouvo Cimento* **2000**, *23*, 1.
[13] W. E. Moerner, S. M. Silence, *Chem. Rev.* **1994**, *94*, 127.
[14] C. M. Lampert, *Thin Solid Films* **1993**, *236*, 6.
[15] *Large-Area Chromogenics: Materials and Devices for Transmittance Control* (Eds: C. M. Lampert, C. G. Granqvist), SPIE Procedings, SPIE, Bellingham, WA **1988**, Vol. IS4.
[16] D. Y. Godovsky, *Adv. Polym. Sci.* **2000**, *153*, 163.
[17] G. Bauer, F. Pittner, T. Schalkhammer, *Mikrochim. Acta* **1999**, *131*, 107.
[18] T. Schalkhammer, *Monatsh. Chem.* **1998**, *129*, 1067.
[19] L. Sheeney-Haj-Ichia, G. Sharabi, I. Willner, *Adv. Funct. Mater.* **2000**, *12*, 27.
[20] S. T. Selvan, T. Hayakawa, M. Nogami, M. Moller, *J. Phys. Chem. B* **1999**, *103*, 7441.
[21] V. Pardo-Yissar, T. Bourenko, J. Wasserman, I. Willner, *Adv. Mater.* **2002**, *14*, 670.
[22] A. C. Khazraji, S. Hotchandani, S. Das, P. V. Kamat, *J. Phys. Chem. B* **1999**, *103*, 4693.
[23] Y. Gotoh, R. Igarashi, Y. Ohkoshi, M. Nagura, K. Akamatsu, S. Deki, *J. Mater. Chem.* **2000**, *10*, 2548.
[24] L. H. Mascaro, E. K. Kaibara, L. O. Bulhoes, *J. Electrochem. Soc.* **1997**, *144*, L273.
[25] G. L. Collins, N. W. Thomas, *J. Polym. Sci.* **1977**, *15*, 1819.
[26] E. Katz, A. L. De Lacey, J. L. G. Fierro, J. M. Palacios, V. M. Fernandez, *J. Electroanal. Chem.* **1993**, *358*, 247.
[27] R. Gabai, N. Sallacan, V. Chegel, T. Bourenko, E. Katz, I. Willner, *J. Phys. Chem. B* **2001**, *105*, 8196.
[28] E. Gileadi, V. Tsionsky, *J. Electrochem. Soc.* **2000**, *147*, 567.
[29] J. D. Jackson, *Classical Electrodynamics*, 2nd ed., Wiley, New York **1975**.
[30] For comparison, the conductivity of copper calculated from the dielectric constant at wavelength 570 nm is equal to 4×10^4 S m^{-1} and the conductivity of bulk copper is ca. 6×10^7 S m^{-1}. Data for the dielectric constant were taken from *Handbook of Optical Constant of Solids* (Ed: E. D. Palik), Academic, New York **1985**.
[31] T. Sosebee, M. Giersig, A. Holzwarth, P. Mulvaney, *Ber. Bunsenges. Phys. Chem.* **1995**, *99*, 40.
[32] G. Lenz, B. J. Eggleton, C. K. Madsen, R. E. Slusher, *IEEE J. Quantum Electron.* **2001**, *37*, 525.
[33] C. Gorecki, *Optoelectron. Rev.* **2001**, *9*, 248.
[34] F. Cacialli, *Philos. Trans. R. Soc. A* **2000**, *358*, 173.
[35] C. G. Granqvist, A. Azens, A. Hjelm, L. Kullman, G. A. Niklasson, D. Ronnow, M. S. Mattsson, M. Yeszelei, G. Vaivars, *Sol. Energy* **1998**, *63*, 199.
[36] G. V. Beketov, Y. M. Shirshov, O. V. Shynkarenko, V. I. Chegel, *Sens. Actuators B* **1998**, *48*, 432.
[37] V. Chegel, O. Raitman, E. Katz, R. Gabai, I. Willner, *Chem. Commun.* **2001**, 883.
[38] O. A. Raitman, E. Katz, A. F. Bückmann, I. Willner, *J. Am. Chem. Soc.* **2002**, *124*, 6487.
[39] E. Katz, D. D. Schlereth, H.-L. Schmidt, *J. Electroanal. Chem.* **1994**, *367*, 59.

Approaching Nanoxerography: The Use of Electrostatic Forces to Position Nanoparticles with 100 nm Scale Resolution

By *Heiko O. Jacobs,* Stephen A. Campbell*, and *Michael G. Steward*

This article reports the directed parallel self-assembly of nanoparticles onto charged surface areas. The charged surface areas were fabricated using a parallel method that employs a flexible, electrically conductive, stamp. The conductive stamp was brought into contact with an 80 nm thick film of poly(methylmethacrylate) (PMMA) supported on n-doped silicon. A voltage pulse between the stamp and the silicon was used to pattern charge in the PMMA thin film electret. Areas as large as 1 cm^2 were patterned with charge at a resolution better than 150 nm in 10 s. These charge patterns attract nanoparticles. The directed self-assembly of nanoparticles from a powder, gas phase (aerosol), and liquid phase (suspension) onto high-resolution charge patterns is demonstrated. The accomplished resolution is 800 nm, which is two orders of magnitude higher than what is achieved by today's xerographic printers.

Nanoparticles can provide a variety of functions and are considered as building blocks of future nanotechnological de-

[*] Prof. H. O. Jacobs, Prof. A. Campbell, M. Steward
Department of Electrical and Computer Engineering
University of Minnesota
200 Union Street SE, Minneapolis, MN (USA)
E-mail: hjacobs@ece.umn.edu

  0935-9648/02/2111-1553 $ 17.50+.50/0

ADVANCED MATERIALS

vices. The ability to assemble nanoparticles in two and three dimensions will enable the fabrication of quantum-effect-based devices. Examples of such devices are single-electron transistors,[1–3] quantum-effect-based lasers,[4,5] photonic band-gap materials, filters, waveguides,[6–8] and high-density data storage.[9–11] The use of nanoparticles as building blocks, however, requires novel assembling strategies. Most actively studied approaches include: i) single particle manipulation,[2,12–16] ii) random particle deposition,[17–19] and iii) parallel particle assembly-based on self-assembly.[7,20–24]

Single-particle manipulation and random particle deposition are useful to fabricate and explore new device architectures. However, inherent disadvantages such as the lag in yield and speed will have to be overcome in the future to enable the manufacturing of nanotechnological devices. Fabrication strategies that rely on mechanisms of self-assembly[6,8,25] may overcome these difficulties. Self-assembly is well known in chemistry and biology, can handle extremely small objects, and is massively parallel, processing large numbers of components simultaneously. The self-assembly occurs due to forces between the objects themselves. We and others have begun to use self-assembly to assemble nanoparticles onto substrates. Current areas of intense investigation use protein recognition,[26–29] DNA hybridization,[22,23,30,31] hydrophobicity/hydrophilicity,[32,33] and magnetic interactions.[10,11,24]

In our own research in this area, we focus on electrostatic interaction because it is long-range and non-material specific (any particle can be trapped).[34] Xerography is the most established example of a printing technique that uses electrostatic force to pattern particles. In xerography, a charge pattern on an appropriate carrier (electret) is used to capture small pigment particles to form an image. The resolution achieved in xerography is about 100 μm.[35–38]

In 1988 Stern et al. demonstrated that a modified atomic force microscope can be used to generate and image charge patterns with ~150 nm resolution.[39] Since then most of the work, including our own, focused on using trapped charges for high-density data storage.[40–42] In 1998 Wright and Chetwynd suggested that such high-resolution charge patterns could be used as templates for self-assembly and as nucleation sites for molecules and small particles.[43] This type of "nanoxerography" has not yet been realized, since high-resolution patterns of charges, extending over large areas, in large quantities, have not been available. The main difficulty is that the fabrication of such charge patterns has been time consuming: the fastest scanning probe-based system needs 1.5 days to pattern an area of 1 cm^2.[42] Multiple tips working in parallel have been suggested.[44–46] It would, however, be more preferable to pattern trapped charges in a single step.

To overcome the lag in speed we recently developed a parallel printing process to pattern charges with ~100 nm resolution.[34] The process uses a flexible, micro-patterned electrode to pattern an electret thin film in a parallel process by injecting and trapping charges over areas of ~1 cm^2 in 10 s. Instead of using a single point contact, we use a conductive flexible stamp to form multiple electric contacts of different size and shape to expose the entire surface in a single step. This patterning approach opens up the route to nanoxerography since it allows the fabrication of charge patterns over large areas in large quantities. Many chips carrying high-resolution charge patterns can be fabricated within an hour, which enables us to study the assembly of different species, inorganic particles, or organic molecules onto charged areas in reasonable timeframes.

In this study, we report on recent improvements in the printing apparatus and demonstrate the use of trapped charge to pattern inorganic nanoparticles from a powder, gas phase (aerosol), and liquid phase (suspension). In each of these cases, the nanoparticles assemble onto the charged areas. In our experiments we achieved a resolution of ~1 μm, which is ~100 times better than the resolution of xerographic copiers.[35–38]

The process to pattern charge is illustrated in Figure 1. A silicon chip coated with a thin film electret was placed on top of a flexible conductive stamp. The stamp forms multiple electric contacts of different size and shape to the rigid surface and was used to electrically expose the selected surface areas. The stamp was poly(dimethylsiloxane) (PDMS), patterned in bas relief using procedures described before;[47] it was ~5 mm thick and supported on a copper plate. The patterned surface of the PDMS stamp was made electrically conducting by ther-

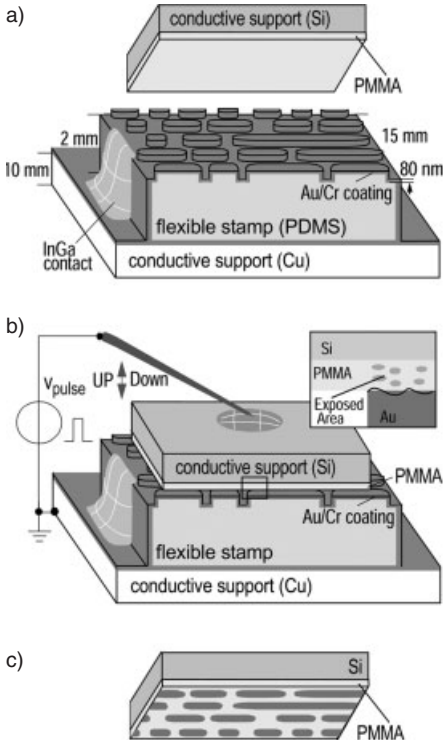

Fig. 1. Principle of parallel charge patterning. a) A thin film of PMMA supported on a doped, electrically conducting Si chip is placed on top of a flexible, gold-coated stamp that is supported on a copper plate. b) A needle, attached to a micromanipulator and connected to an electrometer is brought into contact with the silicon chip. An external voltage is applied between the needle and the copper support to generate a pattern of charge in the PMMA. c) The silicon chip is removed with the PMMA carrying a charge pattern.

  0935-9648/02/2111-1554 $ 17.50+.50/0 *Adv. Mater.* **2002**, *14*, No. 21, November 4

mal evaporation of 80 nm of gold onto it. Thermal expansion of the PDMS stamps during the evaporation can cause the metal coating to buckle on cooling.[48] To prevent buckling due to thermal expansion and contraction of the PDMS stamp, we used eight successive evaporation cycles each 1 min long, with 4 min waiting periods in between for cooling. The copper plates supporting the PDMS stamps were mounted 15 cm away from the metal source in our resistive thermal evaporator (TSH 180H, Pfeiffer/Balzers, Germany). To electrically connect the stamp with the copper plate, we applied InGa (a liquid metal alloy, Aldrich) onto the side walls of the stamp and at the interface between the stamp and the copper plate.

The charge storage medium was poly(methylmethacrylate) (PMMA, an 80 nm film, on a silicon wafer); PMMA is commercially available, and is an electret with good charge storage capabilities.[49] We used a 2 % solution of 950 K PMMA in chlorobenzene (MicroChem Co.) and spin coating at 5000 rpm, to form the film on the wafer. The wafers were <100> n-doped silicon with a resistivity of 3 Ω cm that we cleaned in 1 % solution of hydrofluoric acid to remove the native oxide prior spin coating. The spin-coated PMMA was baked at 90 °C for 1 h under vacuum. The wafer was cut into 1 cm^2 squares. To contact the chips electrically we spread liquid InGa onto the back side of the chip.

We used a metallic needle that is attached to a micromanipulator to contact the liquid InGa on the backside of the chip. Upon contact the InGa wets the needle and forms a low resistance electrical contact. To generate a pattern of trapped charge, we applied an external potential for (1–10 seconds) between the needle and the copper plate. During the exposure we monitored the electric current that followed through the junction and adjusted the voltage (10–30 V) to get ~ 10 mA cm^{-2} exposure current. To lift off the chip after exposure, we made use of the surface tension of the liquid InGa that forms a bond between the silicon and the metallic needle. This bond typically allows us to lift off the chip by retracting the needle using the micromanipulator. In some cases the use of tweezers was required. After lift off, we characterized the charge patterns using Kelvin probe force microscopy (KFM).[50] KFM uses the probe of an atomic force microscope (AFM) to detect electrostatic forces. We developed a KFM procedure that enables us to measure the charge and surface potential distribution with 100 nm scale resolution.[50–53]

To assemble nanoparticles onto charged areas, we investigated three different procedures (Fig. 2). In the first procedure, we dipped PMMA-coated chips carrying a charged pattern into dry powders of nanoparticles and developed the pattern by blowing away the loosely held material in a stream of dry nitrogen. In the second procedure, we exposed chips carrying a charge pattern to a cloud of nanoparticles. The particle cloud was formed inside a cylindrical glass chamber (10 cm in diameter and 5 cm high) using a fan to mix the nanoparticles with the surrounding gas (air or nitrogen). A laser pointer was used to visualize (due to scattering of light) the suspended nanoparticles in the chamber. This particular experiment was used to test whether nanoparticles can be assembled onto charged areas directly from the gas phase. In the third procedure, we used a liquid suspension of nanoparticles. As a solvent we used perfluorodecalin (#601, Sigma-Aldrich, USA), which is a non-polar solvent with a relative dielectric constant of 1.8. To agitate the nanoparticles, we used an ultrasonic bath (Branson 3510, DanBury, CT). In our experiments we used commercially available carbon toner, red iron oxide particles, and graphitized carbon particles.[54]

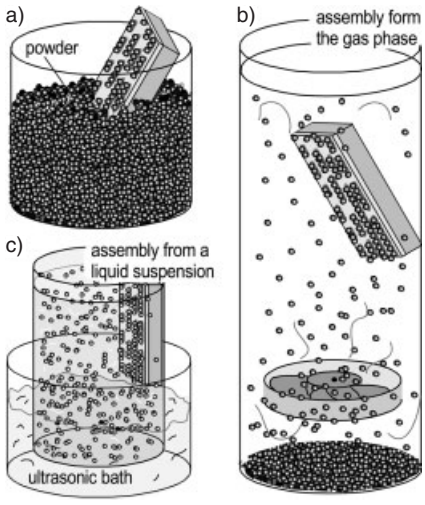

Fig. 2. Illustrations of three different assembly principles. a) The charged chip is immersed into nanoparticle powder. b) The charged chip is exposed to nanoparticles that are suspended in the gas phase. c) The silicon chip is immersed into a solution that contains nanoparticles that are agitated using an ultrasonic bath.

Figure 3 illustrates several representative patterns of localized charge in PMMA that were recorded by KFM. Figure 3a shows the surface potential for a surface patterned in a way that simulates high-density data storage (full width at half maximum (FWHM) < 150 nm, density = 5 Gbits cm^{-2}). The bits are randomly distributed. To write this charge pattern, we exposed the PMMA film with a current density of 20 mA cm^{-2} for 10 s with the metal-coated stamp positive. Figures 3b and 3c show 1 μm sized charged dots and 200 nm (FWHM) wide parallel lines that were written with a current density of 13 mA cm^{-2} for 10 s and 30 mA cm^{-2} for 2 s. The illustrated patterns are representative of those observed over large areas. For the sample illustrated in Figure 3c we have noticed variations in the detected surface potential difference across the surface of the chip. The origin of the variations has not yet been characterized. With clean surfaces and new stamps we are typically able to pattern charge over areas of 1 cm^2. The smallest charge patterns we have generated are about 150 nm in size. At these scales, the transfer function of the Kelvin probe limits the resolution and the patterns are not well resolved.[52] It is important to notice that the amplitudes of the detected potential difference between charged areas and uncharged areas for different samples can not be compared directly. The recorded amplitude depends on the exposure conditions, the size and shape of the charged areas, the condition of the AFM tips, and the sensitivity of the Kelvin probe. These parameters are difficult to keep constant between measurements.

  0935-9648/02/2111-1555 $ 17.50+.50/0

ADVANCED MATERIALS

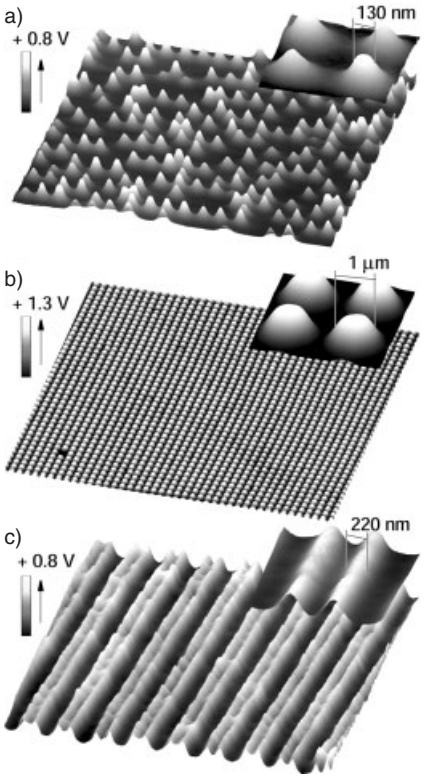

Fig. 3. Kelvin probe force microscopy images of patterns of positive charge. a) Surface potential distribution of a test pattern of high density data storage with < 150 nm-sized bits (FWHM). The pattern was generated using a stamp carrying 150 nm wide circular posts that were 90 nm high. b) Surface potential images of positively charged dots 1 μm in diameter that were generated using circular posts that were 1.4 μm high. c) Surface potential image of 220 nm (FWHM) positively charged parallel lines generated using a stamp carrying 1 μm wide parallel lines that were 900 nm apart, and that were slightly higher at the edge than in the center.

Figure 4 shows representative images of charged based printing using particles from a powder, gas, and liquid phase. The images show patterns of carbon toner (~ 25 μm), red iron oxide (< 500 nm), and graphitized carbon (~ 80 nm) that are trapped at charged areas on PMMA. The resolution achieved was ~ 60 μm for Xerox toner from a powder, ~ 1 μm for red iron oxide particles from a powder, ~ 1 μm for red iron oxide particles from the gas phase, and ~ 800 nm for graphitized carbon from a suspension in perfluorodecalin.

We have not yet determined the actual charge on these particles. In the presented results the different particles were trapped with positive charge patterns. However, we found that the same particles can be trapped with negative charge patterns as well. This phenomenon suggests that the assembly process is dominated by a real charge-induced dipole interaction; i.e., trapped charge in the thin film electret induce a dipole on the particle causing an attractive net force between a polarizable particle and a charged surface area. It is quite remarkable that the trapped charges in the 80 nm thin PMMA film exhibit a sufficient electrostatic force to direct the assembly of the almost three orders of magnitude larger toner particles using the powder method.

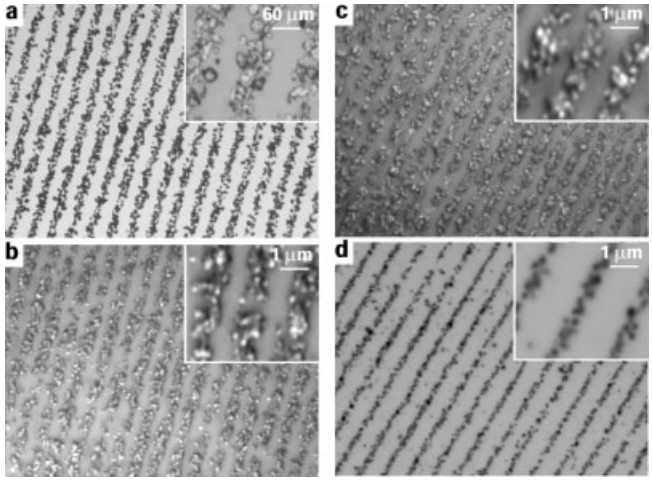

Fig. 4. Optical microscope images of different particles that were assembled from a powder, gas, and liquid phase. a) 60 μm wide parallel lines of toner particles, ~ 25 μm in size, assembled from a powder. b) 1 μm wide parallel lines of red iron oxide particles, < 500 nm in size, assembled from a powder. c) 1 μm wide parallel lines of red iron oxide particles, < 500 nm in size, assembled from the gas phase. d) 800 nm wide parallel lines of graphitized carbon particles, < 100 nm in size, assembled from a liquid phase. In this demonstration, all particles were trapped with positive charge. It was also possible to trap nanoparticles at negative charge patterns.

We demonstrated the directed parallel self-assembly of nanoparticles onto charged surface areas with sub-micrometer resolution. We developed a parallel charge patterning strategy that extends previous serial techniques[40–42] for patterning charge into a parallel method and provides the only parallel method now available for patterning charge in electrets with ~ 100 nm resolution. So far there are many open questions on this patterning process. For example we do not understand the nature of the contact on a molecular level, and the physical nature and location of the trapped charge in the PMMA. However, these charge patterns allow the assembly of particles out of different materials with dimensions ranging from 80 nm–30 μm. The accomplished 800 nm resolution for the 80 nm sized graphite particles is around two orders of magnitude higher than that achieved in traditional xerographic printing. Since it is possible to pattern charge in parallel with ~ 100 nm resolution, higher resolution for the directed self-assembly of nanoparticles might be possible. The evaluation of whether electrostatically directed self-assembly of nanoparticles can be used to assemble nanoparticle based devices will require a number of fundamental studies. For example it is not clear what the ultimate resolution limit of patterned charge is and what experimental conditions are best to achieve particle assembly at charge surface areas. We expect that the assembly process depends on the actual charge on the particle, the electric polarizability of the particle, the thermal energy of the particle, the electric field strength at the substrate surface, the van der Waals interaction between the particles and substrate surface, the suspending medium, and the pressure.

Received: June 20, 2002
Final version: August 1, 2002

  0935-9648/02/2111-1556 $ 17.50+.50/0

[1] M. H. Devoret, R. J. Schoelkopf, *Nature* **2000**, *406*, 1039.
[2] T. Junno, M. H. Magnusson, S. B. Carlsson, K. Deppert, J. O. Malm, L. Montelius, L. Samuelson, *Microelectron. Eng.* **1999**, *47*, 179.
[3] R. J. Schoelkopf, P. Wahlgren, A. A. Kozhevnikov, P. Delsing, D. E. Prober, *Science* **1998**, *280*, 1238.
[4] S. Fafard, K. Hinzer, S. Raymond, M. Dion, J. McCaffrey, Y. Feng, S. Charbonneau, *Science* **1996**, *274*, 1350.
[5] J. Faist, F. Capasso, D. L. Sivco, C. Sirtori, A. L. Hutchinson, A. Y. Cho, *Science* **1994**, *264*, 553.
[6] Y. Xia, B. Gates, Z. Y. Li, *Adv. Mater.* **2001**, *13*, 409.
[7] T. S. Phely-Bobin, R. J. Muisener, J. T. Koberstein, F. Papadimitrakopoulos, *Adv. Mater.* **2000**, *12*, 1257.
[8] D. J. Norris, Y. A. Vlasov, *Adv. Mater.* **2001**, *13*, 371.
[9] H. Brune, M. Giovannini, K. Bromann, K. Kern, *Nature* **1998**, *394*, 451.
[10] C. Petit, A. Taleb, M.-P. Pileni, *Adv. Mater.* **1998**, *10*, 259.
[11] W. L. Zhou, E. E. Carpenter, J. Lin, A. Kumbhar, J. Sims, C. J. O'Connor, *Eur. Phys. J. D* **2001**, *16*, 289.
[12] C. Baur, A. Bugacov, B. E. Koel, A. Madhukar, N. Montoya, T. R. Ramachandran, A. A. G. Requicha, R. Resch, P. Will, *Nanotechnology* **1998**, *9*, 360.
[13] L. T. Hansen, A. Kuhle, A. H. Sorensen, J. Bohr, P. E. Lindelof, *Nanotechnology* **1998**, *9*, 337.
[14] T. J. Krinke, H. Fissan, K. Deppert, M. H. Magnusson, L. Samuelson, *Appl. Phys. Lett.* **2001**, *78*, 3708.
[15] R. Resch, A. Bugacov, C. Baur, B. E. Koel, A. Madhukar, A. A. G. Requicha, P. Will, *Appl. Phys. A* **1998**, *67*, 265.
[16] M. Sitti, H. Hashimoto, *IEEE-ASME Trans. Mech.* **2000**, *5*, 199.
[17] K. Matsumoto, Y. Gotoh, T. Maeda, J. A. Dagata, J. S. Harris, *Jpn. J. Appl. Phys., Part 1* **1999**, *38*, 477.
[18] L. Montelius, T. Junno, S. B. Carlsson, L. Samuelson, *Microelectron. Eng.* **1997**, *35*, 281.
[19] L. Montelius, T. Junno, S. B. Carlsson, M. H. Magnusson, K. Deppert, H. Xu, L. Samuelson, *Microelectron. Reliab.* **1998**, *38*, 943.
[20] D. I. Gittins, D. Bethell, D. J. Schiffrin, R. J. Nichols, *Nature* **2000**, *408*, 67.
[21] W. A. Lopes, H. M. Jaeger, *Nature* **2001**, *414*, 735.
[22] C. M. Niemeyer, *Appl. Phys. A* **1999**, *68*, 119.
[23] C. M. Niemeyer, B. Ceyhan, S. Gao, L. Chi, S. Peschel, U. Simon, *Colloid Polym. Sci.* **2001**, *279*, 68.
[24] Y. Saado, T. Ji, M. Golosovsky, D. Davidov, Y. Avni, A. Frenkel, *Opt. Mater.* **2001**, *17*, 1.
[25] J. H. Fendler, *Chem. Mater.* **2001**, *13*, 3196.
[26] C. Chothia, J. Janin, *Nature* **1975**, *256*, 705.
[27] J. Janin, *Prog. Biophys. Mol. Biol*. **1995**, *64*, 2.
[28] J. T. Moore, P. D. Beale, T. A. Winningham, K. Douglas, *Appl. Phys. Lett.* **1997**, *71*, 1264.
[29] M. J. Dabrowski, J. P. Chen, H. Q. Shi, W. C. Chin, W. M. Atkins, *Chem. Biol.* **1998**, *5*, 689.
[30] E. Braun, Y. Eichen, U. Sivan, G. Benyoseph, *Nature* **1998**, *391*, 775.
[31] P. Malherbe, J. G. Richards, H. Gaillard, A. Thompson, C. Diener, A. Schuler, G. Huber, *Mol. Brain Res.* **1999**, *71*, 159.
[32] I. S. Choi, N. Bowden, G. M. Whitesides, *Angew. Chem. Int. Ed.* **1999**, *38*, 3078.
[33] P. D. Yang, A. H. Rizvi, B. Messer, B. F. Chmelka, G. M. Whitesides, G. D. Stucky, *Adv. Mater.* **2001**, *13*, 427.
[34] H. O. Jacobs, G. M. Whitesides, *Science* **2001**, *291*, 1763.
[35] D. M. Pai, B. E. Springett, *Rev. Mod. Phys.* **1993**, *65*, 163.
[36] R. Groff, P. Khargonekar, D. Koditschek, T. Thieret, L. K. Mestha, in *Proc. of the 38th IEEE Conf. on Decision and Control, Vol. 2*, IEEE, Piscataway, NJ **1999**.
[37] K. Takiguchi, in *Proc. of the 5th International Conf. on High Technology: Imaging Science and Technology*: *Evolution and Promise*, Chiba Univ. Chiba, Japan **1996**.
[38] S. W. Ing, "Xerography—Past, Present, and Future", in *Dig. Technical Papers, SID Int. Symp.* (Ed: J. Morreale), Soc. Inf. Display, Santa Ana, CA **1989**.
[39] J. E. Stern, B. D. Terris, H. J. Mamin, D. Rugar, *Appl. Phys. Lett.* **1988**, *53*, 2717.
[40] R. C. Barrett, C. F. Quate, *Ultramicroscopy* **1992**, *42–44*, 262.
[41] J. E. Stern, B. D. Terris, H. J. Mamin, D. Rugar, *SPIE—Int. Soc. Opt. Eng* **1993**, *1855*, 194.
[42] A. Born, R. Wiesendanger, *Appl. Phys. A* **1999**, *68*, 131.
[43] W. M. D. Wright, D. G. Chetwynd, *Nanotechnology* **1998**, *9*, 133.
[44] K. Wilder, H. T. Soh, A. Atalar, C. F. Quate, *Rev. Sci. Instrum.* **1999**, *70*, 2822.
[45] P. Vettiger, J. Brugger, M. Despont, U. Drechsler, U. Durig, W. Haberle, M. Lutwyche, H. Rothuizen, R. Stutz, R. Widmer, G. Binnig, *Microelectron. Eng.* **1999**, *46*, 11.
[46] P. Vettiger, M. Despont, U. Drechsler, U. Durig, W. Haberle, M. I. Lutwyche, H. E. Rothuizen, R. Stutz, R. Widmer, G. K. Binnig, *IBM J. Res. Dev.* **2000**, *44*, 323.
[47] Y. N. Xia, G. M. Whitesides, *Annu. Rev. Mater. Sci.* **1998**, *28*, 153.
[48] N. Bowden, S. Brittain, A. G. Evans, J. W. Hutchinson, G. M. Whitesides, *Nature* **1998**, *393*, 146.
[49] a) H. S. Nalwa, *Ferroelectric Polymers. Chemistry, Physics and Applications*, Marcel Dekker, New York, **1995**. b) K. Mazur, *J. Phys.* **1997**, *D30*, 1383.
[50] H. O. Jacobs, H. F. Knapp, S. Muller, A. Stemmer, *Ultramicroscopy* **1997**, *69*, 39.
[51] H. O. Jacobs, H. F. Knapp, A. Stemmer, *Rev. Sci. Instrum.* **1999**, *70*, 1756.
[52] H. O. Jacobs, P. Leuchtmann, O. J. Homan, A. Stemmer, *J. Appl. Phys.* **1998**, *84*, 1168.
[53] H. O. Jacobs, A. Stemmer, *Surf. Interface Anal.* **1999**, *27*, 361.
[54] The black toner (product number 13R55) was obtained from Xerox Co., the red iron oxide and graphitized carbon was obtained from PolyScience, Niles, Illinois.

Controllable Fabrication of Aligned Carbon Nanotubes: Selective Position and Different Lengths**

By *Xianbao Wang*, *Yunqi Liu*,* *Ping'an Hu*, *Gui Yu*, *Kai Xiao*, and *Daoben Zhu**

The selective positioning and fabrication of aligned carbon nanotubes[1–3] (CNTs) is particularly important for preparing functional devices such as field emission flat panel displays[4,5] and vacuum microelectronic sources,[6–8] as well as for the development of novel devices. Most of these applications will require a fabrication method capable of producing nanotube alignments or patterns with uniform structures and periodic arrangements in order to meet device requirements. Earlier attempts to manipulate nanotubes for these applications have been made by post-growth methods, such as cutting a polymer resin–nanotube composite,[9] or by drawing a nanotube–ethanol suspension through a ceramic filter.[10] Recently, considerable progress has been made in the fabrication of 2D nanotube alignments, or patterns, using advanced lithographic techniques (for example, photolithography[11–13] and electron beam lithography),[14] micro-contact printing (μCP),[15–17] and shadow masking.[4,18] Patterns prepared in advance can be used to control the architecture of a CNT by acting as either a promoter or inhibitor of the nanotubes' growth. As for the former,[4,12–15,17,19] aligned nanotubes have been grown only in the patterns where catalyst is present: no nanotubes grew on the bare substrate surface. However, for the latter,[11,16,18] nanotubes have been grown on the bare quartz plate, whereas

[*] Prof. Y. Q. Liu, Prof. D. B. Zhu, Dr. X. B. Wang, P. A. Hu, Dr. G. Yu, K. Xiao
Center for Molecular Science, Institute of Chemistry
Chinese Academy of Sciences
Beijing 100 080 (China)
E-mail: liuyq@infoc3.icas.ac.cn

[**] The authors gratefully acknowledge financial support from the National Natural Science Foundation of China (NNSFC), the Major State Basic Research Development Program, and the Chinese Academy of Sciences.

  0935-9648/02/2111-1557 $ 17.50+.50/0